ASEAN
Journal of Scientific and Technological Reports
Online ISSN:2773-8752

Research article

# Detection and Measurement of Natural and Anthropogenic Disturbances in a Protected Area Using the Rasch Model

**Mark Anthony C. Abella[1], and Sherwin E. Balbuena[2*]**

[1] Faculty of Department of Agroforestry, College of Agriculture, Dr. Emilio B. Espinosa Sr. Memorial State College of Agriculture and Technology Main Campus, 5411, Philippines
[2] Faculty of Department of Mathematics, College of Education, Dr. Emilio B. Espinosa Sr. Memorial State College of Agriculture and Technology, Main Campus, 5411, Philippines
* Correspondence: macabella@debesmscat.edu.ph

**Citation:**
Abella, M.A.; Balbuena, S. Detection and Measurement of Natural and Anthropogenic Disturbances in a Protected Area Using the Rasch Model. *ASEAN J. Sci. Tech. Report.* **2026**, 29(3), e260742. https://doi.org/10.55164/ajstr.v29i3.260742.

**Article history:**
Received: August 7, 2025
Revised: November 14, 2025
Accepted: December 3, 2025
Available online: February 27 , 2026



**Abstract:** This study aimed to assess the extent of major threats in the 244.13-hectare Tugbo Natural Biotic Area (TNBA) on Masbate Island, Philippines. Threat-focused patrolling has covered the entire continuum, with a specified recording interval along the protected area (PA), divided into numerous patrol routes. Categorized into human-induced and natural calamities, a total of 27 individual threats were geo-tagged and recorded, with mixed perennial farming as the most frequent threat. Using geo-spatial technologies, the risks were reduced to 10, largely represented by broad expanses of rangelands and invasive monocrop plantations. This paper presents a new methodology for measuring and visualizing threats to protected areas based on the Rasch model. This probabilistic analysis is based on the presence or absence of the threat in each location, disturbance estimates, and the calculation of misfits. The visualization map illustrates that the protected area had an unequal distribution of threats. Most locations have less disturbed areas; hence, the data indicate that the protected area is nearly pristine. This approach is a useful methodology for assessing in-depth environmental disturbance.

**Keywords:** Disturbance; land-use; protected area; rasch model; threats

## 1. Introduction

Changes in land use and land cover (LULC) have become a pressing global environmental concern, driving substantial transformations in ecosystems across tropical regions [1]. The increasing global demand for food production and bioenergy has accelerated these changes, raising alarms over their environmental consequences, particularly in relation to climate change and global warming [2]. Human-driven activities—such as the expansion of agriculture, conflicts between humans and wildlife, infrastructure growth, and mining—intensify pressures on land, posing serious risks to biodiversity and the ecological integrity of natural systems [3]. Biodiversity, which underpins ecosystem resilience and supports human well-being, is under mounting threat from anthropogenic stressors including habitat degradation, overexploitation, pollution, and climate change—contributing to alarming extinction rates [4]. Despite efforts to protect biodiversity through conservation policies and designated protected areas, recent studies suggest that species loss continues, underscoring the ongoing challenges in maintaining ecological balance [5, 6]. In light of these complexities, there is a critical need for research evaluating habitat quality in relation to the diverse, interlinked threats—both human-induced and natural—that affect these dynamic ecosystems.

Geospatial technologies are essential for analyzing land use and land cover (LULC), offering accurate spatial and temporal data for monitoring terrestrial and hydrological dynamics [7]. The use of advanced modeling tools, such as Artificial Intelligence for Environment & Sustainability (ARIES) [8] and Social Values for Ecosystem Services (SoLVES) [9], supports ecological service assessments. However, they often fall short in capturing spatial variability and simulating threat impacts across environmental scenarios [10]. The newly introduced PLUS (Patch-generating Land Use Simulation) model addresses these limitations by integrating machine learning, cellular automata, and spatial policy factors, enabling more realistic LULC simulations—particularly in complex environments such as watersheds and protected areas [11]. The widely used InVEST (Integrated Valuation of Ecosystem Services and Tradeoffs) model offers a robust, spatially explicit framework for habitat quality assessment by integrating temporally dynamic land-use/land-cover data with quantified anthropogenic threat intensities, enabling significant evaluations across transfrontier conservation areas [3, 12] and ecologically sensitive wildlife habitats [13]. Consequently, the CA-Markov hybrid model, which integrates Cellular Automata with Markov Chain analysis, is widely used to simulate and predict spatiotemporal LULC changes in complex watersheds and pasture areas due to its accuracy and efficiency [14, 15]. Recent studies have enhanced this approach by incorporating machine-learning–derived land cover maps as model inputs [16]. Additionally, the CA–Artificial Neural Network model in MOLUSCE offers a more realistic simulation of river basin dynamics by combining spatial patterns and temporal trends within an open-source QGIS framework [17]. The evaluation and prediction of LUCC changes using spatiotemporal data play a vital role in environmental monitoring and in formulating sustainable land management strategies within protected watershed areas.

The introduction of the Rasch probabilistic model [18] is well known for its accuracy and precision in converting categorical item responses to objective-scale measures. It is actually applicable in modern empirical research, often based on parameters from regression models of outcomes represented by a latent variable, such as a person's ability, health, food insecurity, or well-being, as a function of a set of explanatory variables. Simulated data and empirical examples are used to analyze the properties of these processes, demonstrating the utility of the behavioral Rasch selection model for social science study [19]. However, the model has also been successfully used in several applied science studies, demonstrating its practical usefulness across a variety of agricultural and environmental applications. For example, Moral et al. [20] used this method to classify soil fertility potential, map soil production potential, delineate management zones in the field [21], and assess atmospheric pollution levels [22, 23]. While existing LULC modeling frameworks such as PLUS, InVEST, and CA-Markov effectively simulate spatial and temporal transitions in land cover, they operate primarily on deterministic or continuous datasets. These models often assume linearity and visible data inputs, limiting their capacity to represent latent or probabilistic disturbance conditions that arise from overlapping natural and anthropogenic threats [11; 14]. In contrast, the Rasch probabilistic model provides a mathematically rigorous approach for converting dichotomous threat indicators (presence/absence) into a latent continuum of disturbance, expressed in logits [18; 24]. This allows quantifying ecological disturbance as an interval-level construct that integrates multiple independent threat variables into a single, objective scale of environmental pressure [20].

Masbate is an island province in the Philippines, about in the center of the archipelago, between 11°43' north and 123°09' east, and 124°5' east. The province was ranked 9th by the Forest Management Bureau [25], with 6,678 hectares, or 1.17 percent of its total land area, having the least forest cover. Tugbo Natural Biotic Area (TNBA), formerly Tugbo Watershed Forest Reserve (TWFR), was proclaimed under Republic Act No. 11806 in June 2022 as the newest legislated protected area in the country, with a total area of 244.1299 hectares and a length of 19.973 kilometers. It is primarily timberland, with natural forests accounting for more than 50%, while the remaining areas were converted into agricultural and rangeland areas. No comprehensive land-use threat study has been conducted in the watershed, aside from ongoing patrolling and monitoring of the watershed's biodiversity hotspot areas.

There is currently no probabilistic approach that translates qualitative disturbance observations into a statistically validated and reproducible ecological index. By applying the Rasch model, the study introduces a novel analytical framework that integrates spatially heterogeneous field data with psychometric scaling—an innovation rarely applied in ecological or protected-area assessment contexts in the Philippines and Southeast Asia. Information on local-level land-use dynamics is essential for designing sound environmental policies and management. It provides the baseline data required for a proper understanding of how the land was used in the past and the type of changes to be detected in the future [26]. This research, therefore, aimed to visualize the extent of land-use changes across the entire TNBA, using geospatial techniques and a probabilistic model. Specifically, identify and document potential biotic and abiotic threats occurring in the protected area and their spatial distribution; and quantify the magnitude of disturbance using available delineated threat map output and the Rasch model.

## 2. Materials and Methods

### 2.1 Study Area

The research took place at the Tugbo Natural Biotic Area (N 120 18. 974' E 1230 37. 019') within the administrative boundaries of Tugbo, Mobo, Masbate, and Tugbo, Masbate City, Philippines (Figure 1). Land-use data for the watershed were obtained from the Land Management Service (LMS) in Legaspi City, Philippines. The study area has a Type III climate, with dry conditions from November to April and wet conditions the rest of the year. The soil textural classes in the area ranged from clay loam to clayey soil with light to medium brown tones [27]. The landscape varied in elevation from mildly undulating to fairly steep slopes ($5^0$ to $35^0$). The downstream portion of the protected area has a closed canopy, while the middle and upper sections have open, fragmented secondary vegetation with pioneer species.


**Figure 1.** The study area

### 2.2 Disturbance Monitoring Patrol Routes and Sampling Schedule

Data collection was conducted from March to September 2021, covering both the dry (March–June) and wet southwest monsoon (July–September) seasons in the Philippines. This dual-season coverage was designed to capture seasonal variations in disturbance intensity. This period was purposefully selected because both natural disturbances (e.g., landslides, erosion, typhoon-damaged vegetation) and anthropogenic activities (e.g., farming, charcoal-making, tree cutting) are most active and observable during this time. Threat-focused patrolling in the protected area aimed to identify and document disturbances along designated routes systematically, conducted every 1 to 2 weeks per patrol sector. Patrols followed a planned framework ensuring even coverage and appropriate intensity, with threats recorded every 100 meters. Routes extended from the lowermost catchment areas to the upper boundaries of the protected zone, traversing natural divides such as ridges, midslope terrains, and tributaries. Covering an estimated 80 kilometers across 10 routes, all observed threats were recorded and photo-documented for monitoring and management purposes.

### 2.3 Calibrating and Recording Potential Threats

The researcher used a GPS installed in a cellphone and a map of the protected area to record pertinent threats as specified in the module. Each threat was recorded individually by entering the specific name of the potential threat and a brief description, while coordinates, distance covered, and altitude were automatically recorded on the phone.

### 2.4 Ecological Threats in the Protected Area

Environmental threats in TNBA, based on the DENR Lawin Handbook [28], were divided into human-induced and natural calamities. Human-related disturbances include cutting of trees; slash-and-burn farming, hut/house and other infrastructures; annual and perennial farming; a collection of non-timber forest products; charcoal production; wildlife hunting; mining and quarrying; created logging trail; garbage and polluted water; livestock and poultry farming; fire and intentional burning; invasive species while natural phenomena comprise of pest and diseases; landslide and mudslide and typhoon damage.

### 2.5 Mapping of Land-Use Threats

Google Earth Explorer was used to obtain satellite imagery of land use in the watershed, using updated software based on ground geo-tagging. The 2019 base map from the National Mapping and Resource Information Authority (NAMRIA) [29] was used to locate the hotspot area (e.g., land clearing) and to estimate patches of remaining high-value conservation areas in the study site. Existing land cover was computed to include the total area of annual and perennial farmlands, secondary forest, old-growth forest, invasive plantations, and brushlands/grasslands. GPS-equipped devices were used to install waypoints for a particular land cover at irregular intervals across different sections of the watershed. All encircled waypoints were connected to form a polygon that automatically registered the actual area of a sample land cover. To obtain the percentage cover, similar land covers were combined and added to the total land cover, then divided by the total land area of the PA.

### 2.6 Data Analysis

Rasch model (RM) analysis was used to estimate the prevalence of anthropogenic disturbance in the area. Response categories were dichotomized so that the presence or absence of a particular threat was coded as 0 or 1, respectively. Following this collapse of categories, a Dichotomous RM was used, and parameters were estimated using a conditional maximum likelihood procedure in R [30]. Misfit items (threat indicators) were assessed using the Outfit and Infit mean square (MSQ) range 0.7 to 1.3. Further analyses were undertaken to show the item (threat) and person (area) locations along the Wright map and to convert the observed total number of threats to log-odds units (logits). Finally, a heatmap of estimated latent disturbance was visualized using ArcGIS symbology.

## 3. Results and Discussion

### 3.1 Identified Threats at Tugbo Natural Biotic Area

A total of one hundred twenty-five (125) threats from twenty-seven (27) individual threats were recorded during the conduct of the assessment. The majority of the identified and documented threats as stipulated in the Lawin Handbook were observed in the PA, except for wildlife hunting, collection of minor forest products, garbage and polluted water, and livestock and poultry farming, which was observed in TNBA. Unspecified ecological disturbances considered damaging in the PA were added, including orchards, carabao mud pools, and copra drying huts. In addition, human-induced items, such as houses within the PA, were sub-categorized into houses surrounded by crops and animal corrals; likewise, annual farming was separated from perennial farming.

**Table 1.** Summary of environmental threats at TNBA

| Human-induced Threats | Frequency |
|---|---|
| 1. Cutting of trees | 10 |
| 2. Slash-and-burn farming (*kaingin*) | 2 |
| 3. Hut/house within the protected area | 12 |
| 3a. Hut/house surrounded by crops | 10 |
| 3b. Hut/house surrounded by animals/corral | 2 |
| 4. Annual farming | 16 |
| 4a. Open cultivated area planted with a monocrop | 6 |
| 4b. Open cultivated area planted with annual/biennial crops | 10 |
| 5. Mixed perennial farming | 18 |
| 5a. Farming under perennial | 12 |
| 5b. Orchard | 4 |
| 5c.Farming under newly opened/cleared secondary forest | 2 |
| 6. Grazing/barren lands | 11 |
| 7. Abandoned formerly cultivated farmlands | 7 |
| 8. Charcoal production | 5 |
| 9. Post-mining remnants and pits | 5 |
| 10. Logging trail | 4 |
| 11. Intentional fire/burning | 3 |
| 12. Invasive woody species plantation | 8 |
| 13. *Carabao* mud pool | 6 |
| 14. Copra drying hut | 4 |
| SUB-TOTAL | 110 |
| Natural-caused Threats | |
| 15. Pest and diseases | 4 |
| 16. Landslide and mudslide | 8 |
| 17. Typhoon damage to vegetation | 6 |
| SUB-TOTAL | 18 |
| **TOTAL** | **125** |

During the five months of ground validation, mixed perennial farming, the top land-use threat, was categorized into cultivation under established plantations, permanent orchards, and farming under newly opened secondary forest clearings. These were encountered 18 times during intensive reconnaissance in the high forest conservation zone, as cleared patches planted with cash crops. Annual farming was split into open cultivated areas planted with monocrop and open cultivated areas planted with annual/biennial crops. In contrast, mixed perennial farming was divided into farming under perennials, orchards, and farming under newly opened/cleared secondary forests, with 12 farmlands occupying 12.28 hectares tilled by marginalized farmers. During the transect walk, 12 houses/shanties were occupied by families and occasional cultivators scattered in the PA out of more than 20 houses built according to the former Protected Area Superintendent (PASu) and validated during the Socio-Economic Assessment and Monitoring Services (SEAMS) team during their actual household survey in the watershed from August to October 2018 [31]. Combined grasslands and barren domains have a delineated area of 41.59 hectares and have been recorded 11 times across various watershed locations, primarily used for grazing carabao (buffalo) and horses by outside dwellers. Tree cutting was observed 10 times, with a total of 29 trees, including displaced logs, with dbh ranging from 15 to 60 cm, cut within the forest reserve.

**Table 2.** Land cover of TNBA during ground validation

| Land Cover | Area (ha) |
|---|---|
| Secondary forest | 83.70 |
| Barren/grasslands | 67 .69 |
| Invasive perennial trees /orchard plantation | 28.31 |
| Planted native trees | 26.26 |
| Cultivated annual crops | 21.54 |
| Old-growth forest | 16.63 |
| TOTAL | 244.13 |

In the 2020 ground validation result, land use/cover was irregularly distributed within the PA. The NAMRIA-generated map [29] showed that annual crop farmlands occupied the highest land-use with 95.08 has (38.95%), followed by brushlands/grasslands with 72.06 has (29.52%), perennial crops with 58.44 has (23.94%), and grasslands with 6.30 has (2.58%). Patches of grasslands and barren lands (67.69 has, 27.73%), invasive perennial and orchard plantations (28.31 has, 11.60%), and cultivated annual crops (21.54 has, 8.82%) were quantified. Comparing the results of satellite-generated maps and validated ground land use, annual crop cultivation was reduced to 10 percent of the total land area, while barren lands and grasslands were slightly reduced to 10 hectares, owing to effective native tree plantation establishment in the area. Ground validation results provided clearer, more detailed, and updated data on land cover distribution, which may aid local managers in enhancing their current management plans and conservation strategies for the PA.

**3.3 Spatial Grid Framework and Threat Distribution Mapping**

The study area was initially divided into 18 primary grids (1:400 scale) using Google Earth. Each primary grid was further subdivided into 9 secondary grids (1:130 scale), resulting in 162 grid units. To ensure complete coverage of the protected area's irregular boundaries, an additional 8 grids were added. This produced a total of 170 spatial observation units. Each grid unit was considered a "person" in the Rasch model, with binary-coded disturbance data (1 = present, 0 = absent) across ten threat indicators. Plotting the threats involved locating the coordinates of the 10 clustered threats. Each threat within the grid was counted as 1, meaning several threats may be found in a single grid. These factors were clustered into rangelands/barren lands, invasive mono-crop plantation (including orchards), built-up structures (farmhouse, coconut meat drying hut, charcoal production hole and animal mud pool), annual cultivated crops (newly-opened farmlands and open cultivated farms), perennial with annual intercropped (plantation at sapling stage intercropped with annual crops, under coconut and banana plantation intercropping), cutting of trees (timber poaching, sawn timber), uprooted perennial species (damaged by typhoon, pest and diseases infestation), landslide, post-mining remnants and erosion (including open and abandoned farmlands (formerly cultivated areas), slash-and-burn cultivation (intentional setting of fire and forest burning).

At approximately 100 meters from each threat, a total of 170 threats reemerged during the entire validation period. The highest frequency of large rangeland patches occurred in the southeastern part of the Mobo site, which appeared 32 times. Invasive monocrop plantations dominated by large mahogany and gmelina, irregularly planted in the PA, were commonly observed in the north and south sections of Masbate City site, and in some cases in the opposite site. Other major threats that appeared more than 10 times included built-up structures, annual cultivated crops, perennial crops with annual intercropping, and trees or logs cut, while the rest were considered minor disturbances. Except for natural catastrophes, minute structures are visible in the understorey, and ecological threats are vividly evident on Google Earth as concrete evidence of how human beings maltreated the PA.

**Table 3.** Summary of the environmental threat frequency at TNBA

| Threat Indicators | Frequency |
|---|---|
| Rangelands or brushlands (ROB) | 32 |
| Invasive monocrop plantation (IMP) | 31 |
| Built-up structures (BUS) | 24 |
| Annual cultivated crops (ACC) | 24 |
| Perennial with annual intercropped (PAI) | 20 |
| Cutting of trees (COT) | 11 |
| Uprooted perennial species (UPS) | 9 |
| Landslide, post-mining cave-in, and soil erosion (LPS) | 8 |
| Open and abandoned farmland (OAF) | 7 |
| Slash and burn cultivation (SBC) | 4 |
| TOTAL | 170 |

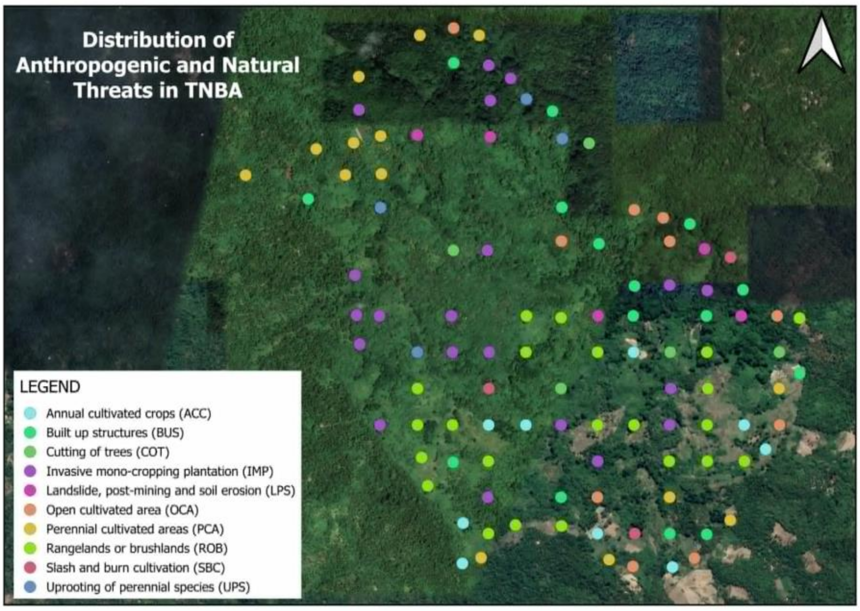


**Figure 2.** GPS-inputted threats at 100-meter distance interval in TNBA

**3.4 Application of the Rasch Model in Measuring the Protected Area Disturbance**

The Rasch model can combine data from multiple variables with different metrics into a single scale of a latent variable. In this study, the various threats observed across locations within the TNBA were consolidated into a single scale, referred to as "forest disturbance". Forest disturbance can be considered a latent variable because it cannot be directly observed. It cannot be observed or measured unless the threats that compose it are found to be present or absent. To prepare the dataset for Rasch analysis, all spatial observations were first converted into binary variables indicating the presence (1) or absence (0) of each threat within every grid unit. Threat intensity was originally recorded on a 0–4 ordinal scale; however, preliminary testing using a Partial Credit Model (PCM) revealed disordered category thresholds, indicating that the ordinal responses did not function sequentially along a single latent continuum of disturbance. When such disordered thresholds occur, recoding into fewer categories or into dichotomous form is recommended to restore proper category functioning and uphold Rasch model assumptions [32, 33]. Accordingly, all non-zero ratings were collapsed into a single "presence" category to reflect better the conceptual aim of detecting whether a disturbance exists at all, an approach also found to improve scale performance in other studies [34,35]. This transformation was implemented to satisfy the requirements of unidimensionality and local independence inherent to Rasch measurement [24]. Following the transformation, model diagnostics were conducted to confirm the appropriateness of the dichotomous specification. A Likelihood Ratio chi-square test showed no significant difference between the PCM and the dichotomous model, $\chi^2(9) = 14.21$, $p = .12$, supporting the simpler dichotomous structure. The dichotomous model exhibited strong measurement precision, with a Person Separation Index (PSI) of 0.82 and item reliability of 0.88 [36]. All threat indicators displayed acceptable fit statistics (infit MSQ 0.876–1.105; outfit MSQ 0.565–1.273), falling within the recommended 0.5–1.5 interval for productive measurement [37]. Threats with fewer than five occurrences across the 170 grids were excluded to avoid unstable parameter estimates, and residual correlations below 0.30 confirmed that the assumption of local independence was met [38]. These diagnostics collectively establish that the dichotomous Rasch model provided a valid and robust basis for estimating watershed disturbance. The line ranges from low to high forest disturbance at each sample location and is operationally defined by the 10 threats. The further to the right a sample point is located, the greater its disturbance (Figure 3). The numerical gradient for this scale is called a logit (log odds) and is established by estimating ordered category threshold parameters for ratings of threat measures that are observed at sampled locations. To estimate threat occurrences and sample location positions, this approach was formally implemented in a dichotomous Rasch model, since the original rating scale (i.e., 0, 1, 2, 3, 4) did not fit the Partial Credit Model due to disordered thresholds. The Rasch analysis in this study is based on the presence (regardless of density) or absence of the threat in each location. It is assumed that the mere presence of destructive human activities in a given location poses an imminent threat to the entire watershed. Using conditional maximum likelihood estimation of the beta and delta parameters in eRm [39], the threat and location disturbance estimates, along with their goodness-of-fit to the Rasch model, were determined. Table 4 presents the threat estimates, their standard errors, and the fit statistics for the threats. The threat estimates ranged from -0.815 to 1.156 logits, indicating that the most frequently observed threat and the rarest are shown in Figure 3. Furthermore, all of the outfit and infit statistics lie between 0.7 and 1.3, except for the outfit of SBC, which lies below the acceptable range. Since the threats did not show consistent misfits (i.e., both outfit and infit are misfits), the data are considered to fit the Rasch model.

**Table 4.** Threat estimates, standard error and Rasch fit statistics

| Threat | Estimate | Std.err | Outfit MSQ | Infit MSQ | Outfit t | Infit t |
|---|---|---|---|---|---|---|
| BUS | -0.815 | 0.212 | 0.887 | 0.935 | -0.793 | -0.486 |
| GOB | -0.77 | 0.215 | 1.11 | 1.09 | 0.783 | 0.709 |
| IMP | -0.725 | 0.218 | 1.076 | 1.05 | 0.542 | 0.406 |
| PCA | -0.213 | 0.259 | 1.273 | 1.105 | 1.226 | 0.588 |
| OCA | 0.023 | 0.283 | 0.961 | 0.975 | -0.073 | -0.035 |
| ACC | 0.114 | 0.294 | 0.862 | 0.943 | -0.453 | -0.164 |
| COT | 0.324 | 0.32 | 0.866 | 0.904 | -0.36 | -0.271 |
| UPS | 0.324 | 0.32 | 0.943 | 0.922 | -0.091 | -0.203 |
| LPS | 0.583 | 0.358 | 0.883 | 0.93 | -0.227 | -0.12 |
| SBC | 1.156 | 0.462 | 0.565 | 0.876 | -0.911 | -0.148 |

**Table 5.** The estimates and standard errors of observed raw scores in the data

| Raw score | Estimate | Standard error |
|---|---|---|
| 0 | Negative infinity | NA |
| 1 | (approx. -3.3897129 as interpolated)<br>-2.3392 | 1.069779 |
| 2 | -1.49443 | 0.811912 |
| 4 | -0.44391 | 0.672329 |

Location disturbance estimates were also calculated. The raw scores, ranging from 0 to 10 (0 indicating the absence of all threats and 10 indicating the presence of all threats), were transformed into Rasch scores in log-odds units (logits). However, only three raw scores were observed in the data: 1, 2, and 4. The other scores were not estimated due to the absence of additional threats at each location; however, a linear interpolation may be performed using the existing information, assuming that the relationship between the raw score and the estimate is nearly linear. (For this study, the estimate for 0 was interpolated.) Furthermore, the Rasch model does not provide estimates for extreme scores (i.e., 0 and 10), as the locations with these raw scores are assumed not to contribute to the measurement. Location misfits were also assessed. Of the 170 locations, only 4 were found to misfit the Rasch model. These are found in Location 66 (12°19'09.66''N, 123°37'22.77''E), Location 91 (12°19'02.67''N, 123°37'24.04''E), Location 112 (12°18'54.01''N, 123°36'53.94''E), and Location 161 (12°18'36.70''N, 123°37'11.35''E). These locations did not show a level of disturbance expected by the Rasch model. In the Wright Map in Figure 3, the distribution of the location disturbance estimates is positively skewed. Most locations have lower disturbance, while only a few have higher disturbance. To visualize the levels of disturbance in the watershed, a heat map was generated in ArcGIS. Before the visualization, the raw score estimates were shifted so that the lowest raw score estimate is zero, to satisfy the software's requirement of a positive weight for each location. This was achieved by dividing the shifted estimate by the sum of the estimates for all 170 locations. The latitude and longitude Together with the weight field, they were converted to a shapefile and uploaded to the GIS software for analysis. The visualization output is shown in Figure 4.

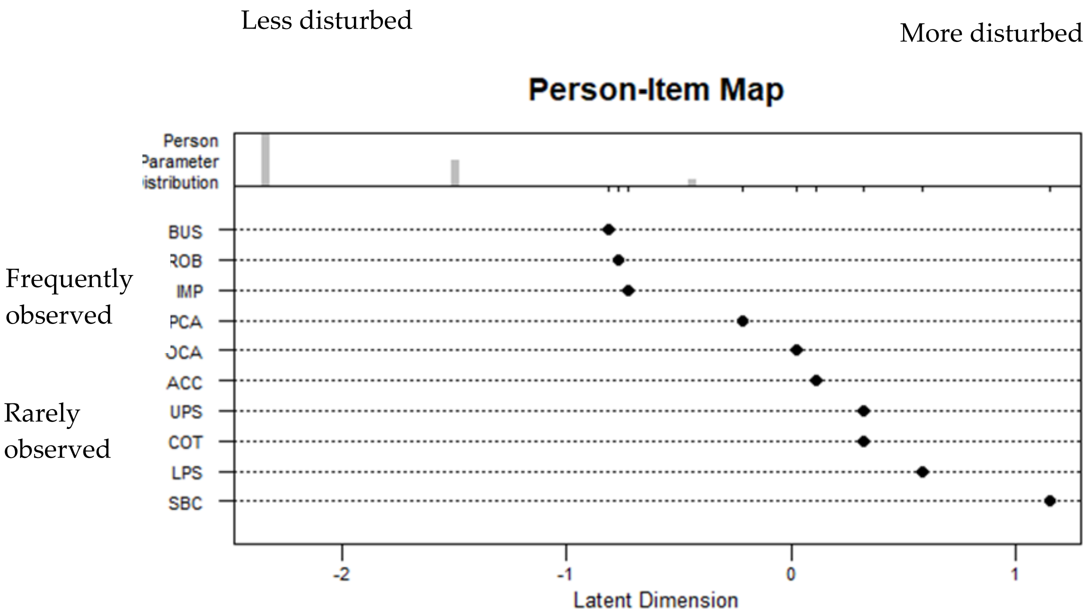


**Figure 3.** Wright map of the threats and locations estimates in TNBA

To improve the spatial accuracy of the visualization, the logit scores derived from the Rasch model were exported to ArcGIS using the centroid coordinates of the 170 grid units, ensuring consistent spatial resolution throughout the protected area. These logits served as weighted attributes for interpolation, enabling the generation of a continuous disturbance surface rather than discrete point observations. Negative logit values (<-2.00) corresponded to low-disturbance zones, aligning with relatively intact forest areas in the northwestern portion of the watershed. In contrast, logit values exceeding +1.00 identified disturbance hotspots concentrated along agricultural edges, grazing lands, and settlement interfaces. This method enhanced mapping precision by converting binary observations into a spatially coherent disturbance gradient, allowing clearer identification of priority zones for management and rehabilitation.

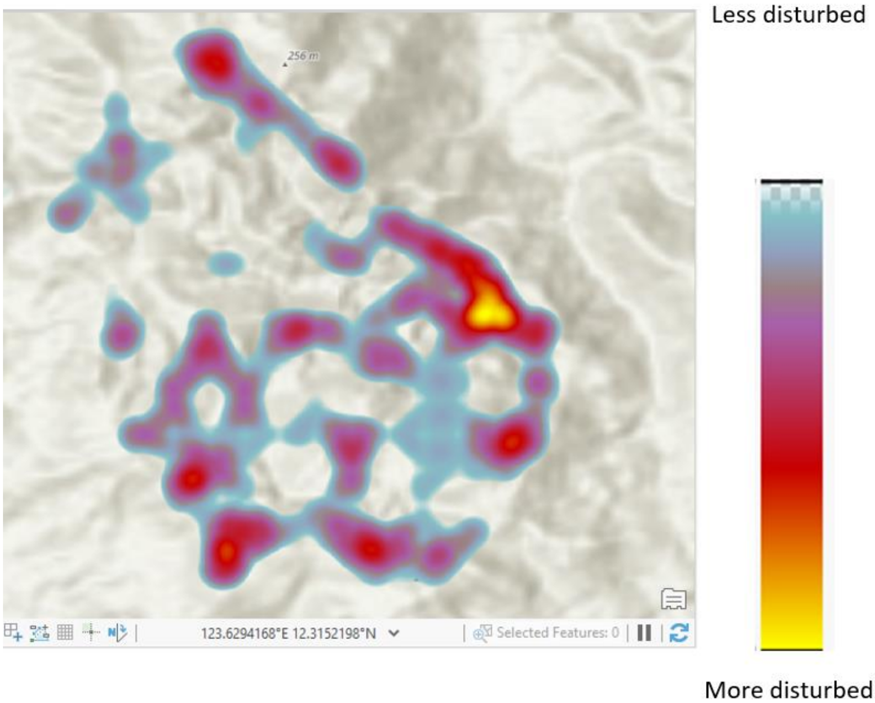


**Figure 4.** Visualization of threat disturbance at TNBA

Locations in the area were colored according to the level of disturbance observed. The absence of color indicates that the area is pristine. The more the color approaches yellow on the spectrum, the greater the disturbance observed in the area. In the heat map, most of the area, especially the northwestern portion, is undisturbed, while greater disturbance was observed along the boundaries and in the lower half of the area. Median comparisons for the Rasch-based disturbance measures between the two areas (lower and upper) showed that the lower portion of the Mobo area has significantly higher disturbance than the upper portion of the Masbate City area. Most grid locations were positioned below -2.00 logits, indicating low overall disturbance, particularly in the northwestern portion of Masbate City. In contrast, higher disturbance scores—typically exceeding +1.00—were observed in the southern Mobo zone, where rangelands, invasive tree plantations, cultivated farms, and built-up structures are more concentrated.

The test for local independence in the Rasch model showed that no pairs of threat items had significant correlations. The magnitude of local independence was calculated from residual item correlations; correlations above 0.3 indicate dependency between items [24]. In theory, significant correlations among the items after removing the influence of the underlying trait (i.e., disturbance) could indicate a violation of the unidimensionality assumption [38]. This means that the threat indicators used to make the latent trait "disturbance" manifest functioned independently but contributed meaningfully to the measurement of that single trait, thereby satisfying one of the important assumptions of the Rasch model.

**Table 6.** Threat item residual correlations

| | ACC | PCA | OCA | IMP | GOB | COT | SBC | BUS | UPS | LPS |
|---|---|---|---|---|---|---|---|---|---|---|
| ACC | 1 | -0.0627 | -0.05838 | -0.19328 | -0.13532 | -0.11944 | 0.193821 | -0.11974 | -0.11302 | -0.09909 |
| PCA | -0.0627 | 1 | -0.11902 | -0.18185 | -0.17856 | -0.10855 | -0.08204 | -0.22448 | -0.10338 | -0.08983 |
| OCA | -0.05838 | -0.11902 | 1 | -0.13994 | -0.13752 | -0.11705 | 0.041018 | -0.18146 | -0.03783 | -0.09707 |
| IMP | -0.19328 | -0.18185 | -0.13994 | 1 | -0.2826 | -0.01362 | -0.13405 | -0.14073 | -0.06901 | -0.14523 |
| GOB | -0.13532 | -0.17856 | -0.13752 | -0.2826 | 1 | -0.11287 | -0.13098 | -0.13642 | -0.1071 | -0.14225 |
| COT | -0.11944 | -0.10855 | -0.11705 | -0.01362 | -0.11287 | 1 | -0.08503 | -0.17045 | -0.0548 | 0.007591 |
| SBC | 0.193821 | -0.08204 | 0.041018 | -0.13405 | -0.13098 | -0.08503 | 1 | -0.05679 | -0.0799 | -0.07039 |
| BUS | -0.11974 | -0.22448 | -0.18146 | -0.14073 | -0.13642 | -0.17045 | -0.05679 | 1 | -0.16174 | 0.030356 |
| UPS | -0.11302 | -0.10338 | -0.03783 | -0.06901 | -0.1071 | -0.0548 | -0.0799 | -0.16174 | 1 | -0.08474 |
| LPS | -0.09909 | -0.08983 | -0.09707 | -0.14523 | -0.14225 | 0.007591 | -0.07039 | 0.030356 | -0.08474 | 1 |

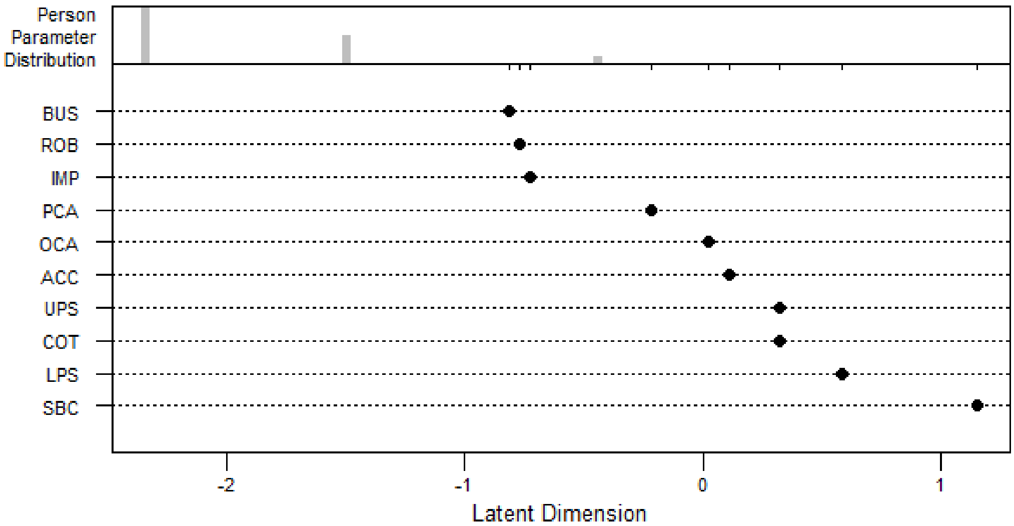


**Figure 5.** Wright Map on the relative positions of the threat items and locations of disturbance in TNBA

Estimating the threat item and location disturbance parameters led to the construction of the Wright Map (Figure 5). This map illustrates the relative positions of the threat items and location disturbance on the same linear scale (latent dimension). The upper portion of the map shows the distribution of the location disturbance estimates (or Person Parameter Distribution). In contrast, the lower portion shows the positions of the threat items based on their estimated severity (frequency or rarity, in this case, with items on the left more frequently observed and those on the right less frequently observed).

As shown in the person parameter distribution, most locations have disturbance estimates below -2.00, compared with the lowest threat item estimate of -0.815. Since the distributions of threat items and location disturbance did not have the same central tendencies, with the former near 0.00 and the latter near -2.00, the probability that a given threat exists at each location is very low. Hence, the watershed is nearly pristine. In this study, the highest threat item estimate for SBC was 1.156; therefore, a location with disturbance estimates equal to or greater than 1.156 can be considered severely disturbed.

**Table 7.** Disturbance scale derived using the threat item estimates

| Location disturbance estimate | | Disturbance level |
|---|---|---|
| Lower limit (in logits) | Upper limit (in logits) | |
| -infinity | -0.815 | Very low |
| -0.815 | 0.1705 | Low |
| 0.1705 | 1.156 | High |
| 1.156 | +infinity | Very high |

## 4. Conclusions

A comprehensive assessment of disturbances within the Tugbo Natural Biotic Area emerges from the combined application of ground validation, GIS techniques, and Rasch probabilistic modeling. Ground surveys remain indispensable for documenting fine-scale threats such as timber extraction, mining remnants, charcoal pits, and pest or disease occurrences—factors that are not consistently detected in GIS-based simulations. When integrated with GIS, these data produce a coherent spatial representation of disturbance intensity across the landscape. The Rasch model contributes an innovative measurement component by converting categorical observations into interval-level logits, providing a consistent and objective disturbance index. This triangulated methodology strengthens the scientific basis for adaptive management, enabling protected area managers to identify priority zones and implement targeted conservation interventions. This study confirms that the Tugbo Natural Biotic Area is not entirely pristine but remains largely intact, with localized zones of moderate anthropogenic disturbance. The integration of the Rasch model with GIS offers a novel approach to environmental monitoring by converting qualitative field observations into quantitative interval-level disturbance measures, enabling a more objective evaluation than traditional descriptive or remote–sensing–only approaches. These results can support the Protected Area Management Board in identifying disturbance hotspots, prioritizing zones for rehabilitation, allocating patrolling and monitoring resources more efficiently, and establishing a standardized, repeatable assessment protocol using the same 170-grid framework for long-term ecological monitoring.

## 5. Acknowledgements

The main author sincerely thanks the K-12 program of the Commission on Higher Education (CHED) for the award of its full scholarship and for providing it with financial support for this report. He also acknowledges DENR RO V, CENRO–Mobo, and the TNBA–PAMB for granting authorization to undertake this research in the protected area. Special mention to Dr. Sherwin E. Balbuena, his co-author and statistician, for conceptualizing the study using the Rasch model, which enabled visualization of environmental disturbance.

**Author Contributions:** The following are the contributions of each author in this research: Conceptualization: Abella, MAC and Balbuena, SE; Methodology: Abella, MAC and Balbuena, SE; Software: Balbuena, SE; Validation: Abella, MAC; Formal analysis: Balbuena, SE; Investigation: Abella, MAC; Resources: Abella, MAC; Data curation: Balbuena, SE and Abella, MAC; Writing—original draft preparation: Abella, MAC; Writing—review and editing: Abella, MAC and Balbuena, SE; Visualization: Balbuena, SE and Abella, MAC; Supervision: Abella, MAC; Project administration: Abella, MAC; and Funding acquisition: Abella, MAC.

**Funding:** The main author received a CHED K-12 scholarship.

**Conflicts of interest:** The authors declare no conflict of interest.

## References

[1] Solaimani, K.; Darvishi, S. Comparative Analysis of Land Use Changes Modeling Based-on New Hybrid Models and CA-Markov in the Urmia Lake Basin. *Adv. Space Res.* **2024**, *74*(8), 3749–3764. https://doi.org/10.1016/j.asr.2024.06.078

[2] Roy, P. S.; Ramachandran, R. M.; Paul, O.; Thakur, P. K.; Ravan, S.; Behera, M. D.; Kanawade, V. P. Anthropogenic Land Use and Land Cover Changes—A Review on Its Environmental Consequences and Climate Change. *J. Indian Soc. Remote Sens.* **2022**, *50*(8), 1615–1640. https://doi.org/10.1007/s12524-022-01569-w

[3] Nyathi, N. A.; Musakwa, W.; Krenz, J.; Kuhn, N. J. Spatio-Temporal Dynamics of Habitat Quality Explored with InVEST: The Case of the Greater Limpopo Transfrontier Conservation Area. *Sustain. Environ.* **2025**, *11*(1), 2520642. https://doi.org/10.1080/27658511.2025.2520642

[4] Batool, S.; et al. Nature's Comeback: Case Studies of South Asian Countries Regarding Biodiversity Restoration and Conservation. In *Sustainable Synergy: Harnessing Ecosystems for Climate Resilience*; Choudhury, M., Dixit, G., Majumdar, S., Eds.; Climate Change Management; Springer: Cham, 2025. https://doi.org/10.1007/978-3-031-77957-2_5

[5] Pulido-Chadid, K.; Virtanen, E.; Geldmann, J. How Effective Are Protected Areas for Reducing Threats to Biodiversity? A Systematic Review Protocol. *Environ. Evid.* **2023**, *12*(1). https://doi.org/10.1186/s13750-023-00311-4

[6] Meng, Z.; Dong, J.; Ellis, E. C.; Metternicht, G.; Qin, Y.; Song, X.-P.; Löfqvist, S.; Garrett, R. D.; Jia, X.; Xiao, X. Post-2020 Biodiversity Framework Challenged by Cropland Expansion in Protected Areas. *Nat. Sustain.* **2023**, *6*(7), 758–768. https://doi.org/10.1038/s41893-023-01093-w

[7] Girma, R.; Fürst, C.; Moges, A. Land Use Land Cover Change Modeling by Integrating Artificial Neural Network with Cellular Automata-Markov Chain Model in Gidabo River Basin, Main Ethiopian Rift. *Environ. Chall.* **2022**, *6*, 100419. https://doi.org/10.1016/j.envc.2021.100419

[8] Wang, J.; Wu, Y.; Gou, A. Habitat Quality Evolution Characteristics and Multi-Scenario Prediction in Shenzhen Based on PLUS and InVEST Models. *Front. Earth Sci.* **2023**, *11*. https://doi.org/10.3389/fenvs.2023.1146347

[9] Chen, C.; Liu, J.; Bi, L. Spatial and Temporal Changes of Habitat Quality and Its Influential Factors in China Based on the InVEST Model. *Forests* **2023**, *14*(2), 374. https://doi.org/10.3390/f14020374

[10] Sun, J.; Ongsomwang, S. Optimal Parameters of Random Forest for Land Cover Classification with Suitable Data Type and Dataset on Google Earth Engine. *Front. Earth Sci. (Lausanne)* **2023**, *11*. https://doi.org/10.3389/feart.2023.1188093

[11] Li, X.; Liu, Z.; Li, S.; Li, Y. Multi-Scenario Simulation Analysis of Land Use Impacts on Habitat Quality in Tianjin Based on the PLUS Model Coupled with the InVEST Model. *Sustainability* **2022**, *14*(11), 6923. https://doi.org/10.3390/su14116923

[12] Admasu, S.; Yeshitela, K.; Argaw, M.; Bloor, M. Assessing Habitat Quality Using the InVEST Model in the Dire and Legedadi Watersheds, Central Highland of Ethiopia: Implication for Watershed Management. *Sustain. Environ.* **2023**, *9*(1). https://doi.org/10.1080/27658511.2023.2242137

[13] Nematollahi, S.; Fakheran, S.; Kienast, F.; Jafari, A. Application of InVEST Habitat Quality Module in Spatially Vulnerability Assessment of Natural Habitats (Case Study: Chaharmahal and Bakhtiari Province, Iran). *Environ. Monit. Assess.* **2020**, *192*(8). https://doi.org/10.1007/s10661-020-08460-6

[14] Tahir, Z.; Haseeb, M.; Mahmood, S. A.; Batool, S.; Abdullah-Al-Wadud, M.; Ullah, S.; Tariq, A. Predicting Land Use and Land Cover Changes for Sustainable Land Management Using CA-Markov Modelling and GIS Techniques. *Sci. Rep.* **2025**, *15*(1), 3271. https://doi.org/10.1038/s41598-025-87796-w

[15] Dos Santos, W. P.; Acuña-Guzman, S. F.; de Oliveira, P. T.; Beniaich, A.; Cardoso, D. P.; Silva, M. L.; Avanzi, J. C. CA-Markov Prediction Modeling for the Assessment of Land Use/Land Cover Change in Two Sub-Basins of the Tocantins-Araguaia River Basin. *Environ. Monit. Assess.* **2024**, *196*(6), 499. https://doi.org/10.1007/s10661-024-12673-4

[16] Hakim, A. M. Y.; Santosa, B. H.; Martono, D. N.; Sencaki, D. B.; Prayogi, H.; Arifandri, R.; Steinhausen, M. J. Exploring Land Cover Change Impacts on Ecosystem Services Using Machine Learning Technique and Scenario Simulation: Case Study of the Upper Citarum River Basin, Indonesia. *Mod. Earth Syst. Environ.* **2025**, *11*(3), 211. https://doi.org/10.1007/s40808-025-02352-9

[17] Blissag, B.; Yebdri, D.; Kessar, C. Spatiotemporal Change Analysis of LULC Using Remote Sensing and CA-ANN Approach in the Hodna Basin, NE of Algeria. *Phys. Chem. Earth, Parts A/B/C* **2024**, *133*, 103535. https://doi.org/10.1016/j.pce.2023.103535

[18] Loyd, B. H.; Hoover, H. D. Vertical Equating Using the Rasch Model. *J. Educ. Meas.* **1980**, *17*(3), 179–193.

[19] Rabbitt, M. P. Causal Inference with Latent Variables from the Rasch Model as Outcomes. *Measurement* **2018**, *120*, 193–205. https://doi.org/10.1016/j.measurement.2018.01.044

[20] Moral, F. J.; Terrón, J. M.; Rebollo, F. J. Site-specific Management Zones Based on the Rasch Model and Geostatistical Techniques. *Comput. Electron. Agric.* **2011**, *75*(2), 223–230. https://doi.org/10.1016/j.compag.2010.10.014

[21] Moral, F. J.; Rebollo, F. J.; Terrón, J. M. Analysis of Soil Fertility and Its Anomalies Using an Objective Model. *J. Plant Nutr. Soil Sci.* **2012**, *175*(6), 912–919. https://doi.org/10.1002/jpln.201100361

[22] Moral, F. J.; Álvarez, P.; Canito, J. L. Mapping and Hazard Assessment of Atmospheric Pollution in a Medium Sized Urban Area Using the Rasch Model and Geostatistics Techniques. *Atmos. Environ.* **2006**, *40*(8), 1408–1418. https://doi.org/10.1016/j.atmosenv.2005.10.054

[23] Moral, F. J.; Rebollo, F. J.; Valiente, P.; López, F. Modeling of Atmospheric Pollution in Urban and Rural Sites Using a Probabilistic and Objective Approach. *Appl. Sci.* **2019**, *9*(19), 4009. https://doi.org/10.3390/app9194009

[24] Tennant, A.; Conaghan, P. G. The Rasch Measurement Model in Rheumatology: What Is It and Why Use It? When Should It Be Applied, and What Should One Look for in a Rasch Paper? *Arthritis Care Res.* **2007**, *57*(8), 1358–1362. https://doi.org/10.1002/art.23108

[25] Forest Management Bureau. Top 10 Most Deforested Provinces in the Philippines. *Philippine Forest Cover*. Philstar, March 4, **2018**. https://www.philstar.com/headlines/2018/03/04/1793446/recovering-philippines-forest-cover (accessed 2026-02-23).

[26] Estoque, R. C.; Murayama, Y.; Lasco, R. D.; Myint, S. W.; Pulhin, F. B.; Wang, C.; Hijioka, Y. Changes in the Landscape Pattern of the La Mesa Watershed—The Last Ecological Frontier of Metro Manila, Philippines. *For. Ecol. Manage.* **2018**, *430*, 280–290. https://doi.org/10.1016/j.foreco.2018.08.023

[27] Regional Soils Laboratory. *Soil Test Result Interpretation*; Integrated Laboratory Division, DA-RFU ROV: Naga City, Philippines, **2019**.

[28] Forest Management Bureau. *LAWIN Forest and Biodiversity Protection System. Module 2: Purpose-driven Patrolling*; Forest Conservation Area Planning: **2018**. http://pdf.usaid.gov (accessed 2026-02-23).

[29] National Mapping and Resource Information Authority. *Land Cover Map of Tugbo Watershed Forest Reserve, Province of Masbate*; Land Mapping Division: Legaspi City, Philippines, **2019**.

[30] Mair, P.; Hatzinger, R. CML Based Estimation of Extended Rasch Models with the eRm Package in R. *Psychol. Sci.* **2007**, *49*(1), 26–43.

[31] Provincial Environment and Natural Resources – Community Environment and Natural Resources Office. *Socio-economic Assessment Monitoring System (SEAMS). Tugbo Watershed Forest Reserve*; Masbate City, Philippines, **2018**.

[32] Bond, T. G.; Fox, C. M. *Applying the Rasch Model: Fundamental Measurement in the Human Sciences*, 3rd ed.; Routledge: New York, **2015**.

[33] Boone, W. J.; Staver, J. R.; Yale, M. S. *Rasch Analysis in the Human Sciences*; Springer: Dordrecht, **2014**.

[34] Tsai, C. L.; Wind, S.; Estrada, S. Exploring the Effects of Collapsing Rating Scale Categories in Polytomous Item Response Theory Analyses: An Illustration and Simulation Study. *Meas.: Interdiscip. Res. Perspect.* **2025**, *23*(1), 66–89.

[35] Quan, Y.; Wang, C. Collapsing or Not? A Practical Guide to Handling Sparse Responses for Polytomous Items. *Methodology* **2025**, *21*(1), 46–73.

[36] Linacre, J. M. *Winsteps Rasch Measurement Computer Program User's Guide*, Version 5.1.1; Winsteps.com: **2021**.

[37] Linacre, J. M. What Do Infit and Outfit, Mean-Square and Standardized Mean. *Rasch Meas. Trans.* **2002**, *16*(2), 878.

[38] Lee, Y. W. Examining Passage-related Local Item Dependence (LID) and Measurement Construct Using Q3 Statistics in an EFL Reading Comprehension Test. *Lang. Test.* **2004**, *21*(1), 74–100. https://doi.org/10.1191/0265532204lt260oa

[39] Mair, P.; Hatzinger, R. CML-based Estimation of Extended Rasch Models with the eRm Package in R. *Psychol. Sci.* **2007**, *49*(1), 26–43.